

Development of an Extended Compact Crack Arrest Specimen

R.E. Link,¹

¹ *U.S. Naval Academy, Annapolis, MD, USA*
E-mail: *link@usna.edu*

The compact crack arrest specimen is the standard specimen geometry used for crack arrest testing in ASTM E1221. Many crack arrest tests are invalid because of crack branching or otherwise leaving the intended crack plane during rapid crack propagation. An extended compact specimen geometry was developed to decrease the magnitude of the positive T-stress and improve the crack path stability. Finite element analysis was performed to determine a suitable compliance calibration of the specimen and to characterize the T-stress in the new specimen. Results of the compliance calibration and the experimental validation are presented. The T stress was reduced by 50% in the new specimen compared with the standard compact specimen. A series of crack arrest tests were performed using the standard compact crack arrest specimen and the extended specimen geometry.

1.0 Introduction

ASTM standard test method E1221, Standard Test Method for Determining Plane-Strain Crack-Arrest Fracture Toughness, K_{Ia} , of Ferritic Steels specifies a wedge-loaded, compact crack arrest specimen for use measuring the crack arrest fracture toughness [1]. It can be difficult to achieve valid test results using this test method because of problems initiating a cleavage crack, achieving crack arrest within the test section and crack branching or deviation from the intended crack plane [2][3]. The overall success rate during a round-robin test program conducted as part of the standard development process was about 50% [4]. A typical example of severe crack path deviation that can be observed is shown in Figure 1. The tendency for the crack to leave the crack plane is believed to be a consequence of a large, positive T-stress present in the CCA specimen. The single edge-notch tension, SE(T), specimen, which has a negative T-stress, does not have this problem.

The wedge-loaded CCA specimen geometry has several desirable characteristics as a crack arrest specimen compared with the SE(T) specimen. The absolute specimen size is relatively small, under wedge-loading it has a decreasing K-field with crack growth and the test procedure is relatively simple. The test method described in ASTM E1221 employs a quasi-static analysis of the CCA specimen together with a measurement of crack-mouth opening displacement immediately after crack arrest to estimate the crack arrest fracture toughness. It has been demonstrated that this approach yields slightly conservative estimates of the true crack arrest fracture toughness [4][5]. This assumption is not true for all specimen geometries. The double cantilever

specimen and the SE(T) specimen both exhibit significant dynamic effects that preclude the use of a quasi-static analysis for those specimens [6][7]

The objective of this investigation was to develop a specimen that maintains the desirable attributes of the CCA specimen while reducing the T-stress.



Figure 1 Compact crack arrest specimen with crack growing out of intended crack plane.

2.0 Extended Compact Crack Arrest Specimen

The positive T stress in the CCA specimen is largely a consequence of the bending stress field that develops in the specimen arms. The bending stress field can be reduced by increasing the bending stiffness of the arms. An extended compact crack arrest specimen geometry is shown in Figure 2. The specimen is 60% larger than a CCA specimen with the same width. Increasing the size of the specimen arms by a factor of 1.6 increases the stiffness of the arms by a factor of approximately four. The specimen is loaded by using a wedge to drive a split pin placed in the hole on the crack line. The pair of holes remote from the crack line are provided so that the specimen notch may be fatigue precracked if desired.

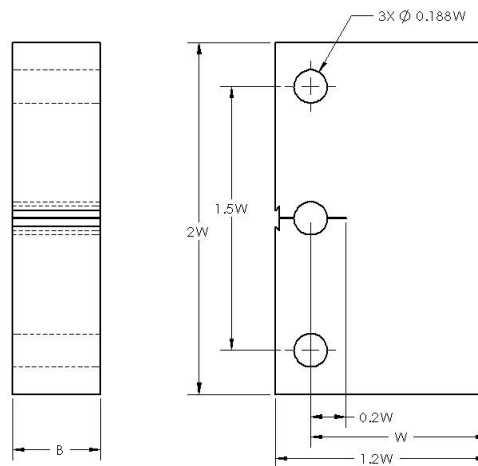


Figure 2 Schematic drawing of the extended compact crack arrest (ECCA) specimen.

3.0 Finite Element Analysis

Finite element analysis was used to calculate the stress intensity factor and compliance relationships necessary for determining the crack initiation and arrest toughness using the ECCA specimen. Linear-elastic, plane strain finite element models with crack sizes ranging from $0.265 \leq a/W \leq 0.9$ were analyzed. The research finite element code, WARP3D, was used to perform the analyses [8]. The stress intensity factor and the T stress were determined using the interaction integral computational capability within WARP3D. Two different loading configurations of the ECCA specimen were analyzed: the remote pin-loaded configuration for specimen precracking and the crack-line, wedge-loaded configuration for crack arrest testing.

3.1 Pin-loaded configuration

The plane strain, finite element model used for these analyses is shown in Figure 3. The model used a single layer of 8-node brick elements with plane strain conditions applied to the faces of the model by constraining the out-of-plane displacement of the nodes. The model had 3613 elements and 7443 nodes. A focused mesh was employed at the crack tip. The pin-loading was modeled by applying displacements to the nodes in the model corresponding to the location of the center of the pin. The pin-holes were not explicitly modeled.

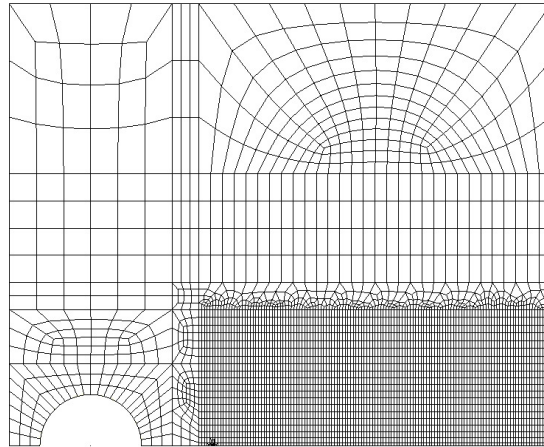


Figure 3 Plane strain finite element mesh of one half of the ECCA specimen.

A calibration of the specimen compliance is necessary for estimating the crack size from compliance measurements during precracking. The normalized crack size, a/W , is plotted in Figure 4 as a function of the normalized specimen compliance, u where:

$$u = \frac{1}{\left[\left(E'B \sqrt{P} \right)^{1/2} + 1 \right]}$$

with

$$E' = \frac{E}{(1-\nu^2)},$$

E = elastic modulus,

ν = Poisson's ratio,

B = specimen thickness,

v = crack mouth opening displacement measured at the specimen edge, and

P = force applied to the specimen.

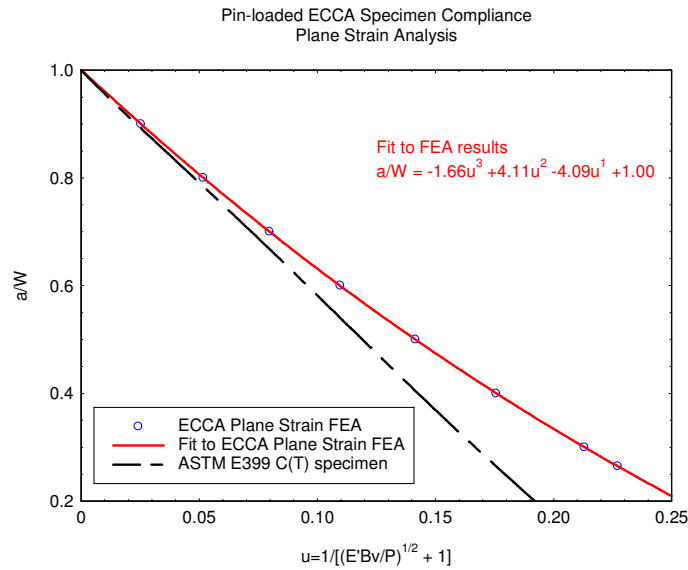


Figure 4 Crack length as a function of normalized specimen compliance for the pin-loaded ECCA specimen compared with the standard compact specimen.

Also shown in the figure is the compliance expression for the standard pin-loaded C(T) specimen from ASTM E399 [9]. The increased bending stiffness of the ECCA specimen is evident from the figure.

The stress intensity factor, K, for the pin-loaded, ECCA specimen is:

$$K = \frac{P}{B\sqrt{W}} f\left(\frac{a}{W}\right)$$

where

$$f\left(\frac{a}{W}\right) = \frac{\left(2 + \frac{a}{W}\right) \left[1.03 + 1.08 \frac{a}{W} - 1.71 \left(\frac{a}{W}\right)^2 + 0.692 \left(\frac{a}{W}\right)^3\right]}{\left(1 - \frac{a}{W}\right)^{3/2}}.$$

The $f(a/W)$ function is plotted in Figure 5 along with the similar function for the standard C(T) specimen. The ECCA function is slightly below the C(T) function over the full range of crack sizes.

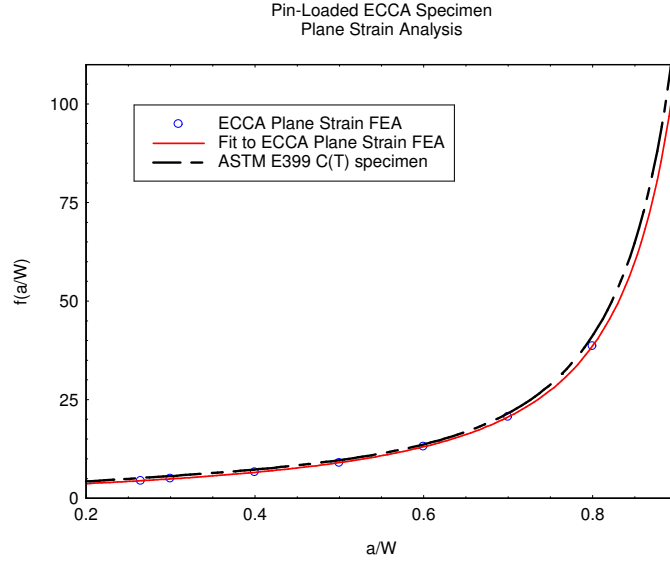


Figure 5 Stress intensity factor $f(a/W)$ functions for the pin-loaded ECCA and the compact specimen.

3.2 Wedge-loaded configuration

The finite element analysis of the wedge-loaded ECCA specimen utilized the same model as the pin-loaded configuration except that the model was loaded by applying displacements to the boundary of the hole along the crack line to simulate the displacements from the split-pin. The stress intensity factor for the ECCA specimen as a function of the crack mouth opening displacement, δ , measured at the edge of the specimen is given by:

$$K = \frac{E\delta \sqrt{B/B_N}}{\sqrt{W}} f_{\delta} \left(\frac{a}{W} \right)$$

where

$$f_{\delta} \left(\frac{a}{W} \right) = \left(2 + \frac{a}{W} \right)^{1/2} \left[1.00 - 3.17 \frac{a}{W} + 5.98 \left(\frac{a}{W} \right)^2 - 5.54 \left(\frac{a}{W} \right)^3 + 1.96 \left(\frac{a}{W} \right)^4 \right]$$

and

B_N = net specimen thickness for a sidegrooved specimen.

The $f_{\delta}(a/W)$ function for the ECCA specimen is compared with the similar function for the standard CCA specimen in Figure 6.

The stress intensity factor as a function of crack length for a CCA and an ECCA specimen loaded to the same initial stress intensity, K_o , under fixed displacement conditions which are approximated by the wedge-loaded configuration is plotted in Figure 7. The crack driving force decays at a faster rate in the ECCA specimen than in the CCA specimen over the range of practical crack lengths in a crack arrest test. This behavior should favor crack arrest in the ECCA specimen at a shorter crack length than in the CCA specimen.

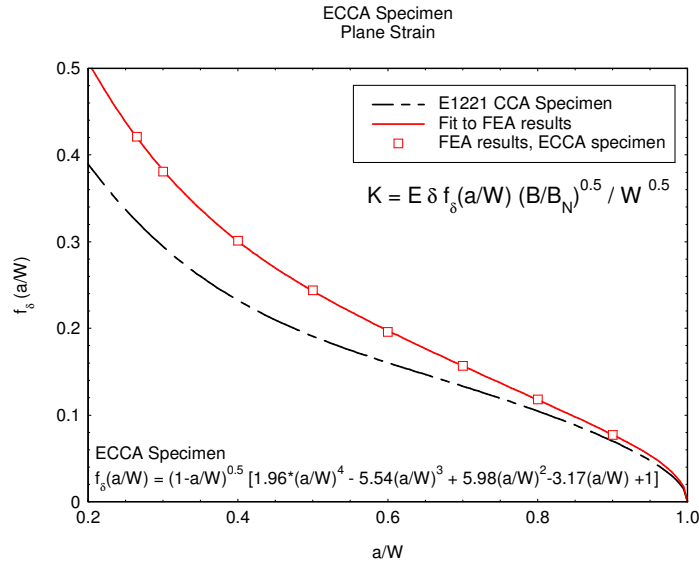


Figure 6 Comparison of the displacement-based geometry correction factor, f_δ , for the E1221 compact crack arrest specimen and the ECCA specimen.

The normalized T-stress variation in the wedge-loaded, ECCA specimen is compared with the standard pin-loaded C(T) specimen and the SE(T) specimen in Figure 8. Also shown in the figure are calculations performed in this investigation of the normalized T stress for the wedge-loaded CCA specimen. The ECCA specimen has a significantly lower T stress than the CCA specimen over the full range of crack lengths. For $a/W \leq 0.5$, the T stress in the ECCA specimen is approximately 50% less than in the CCA specimen.

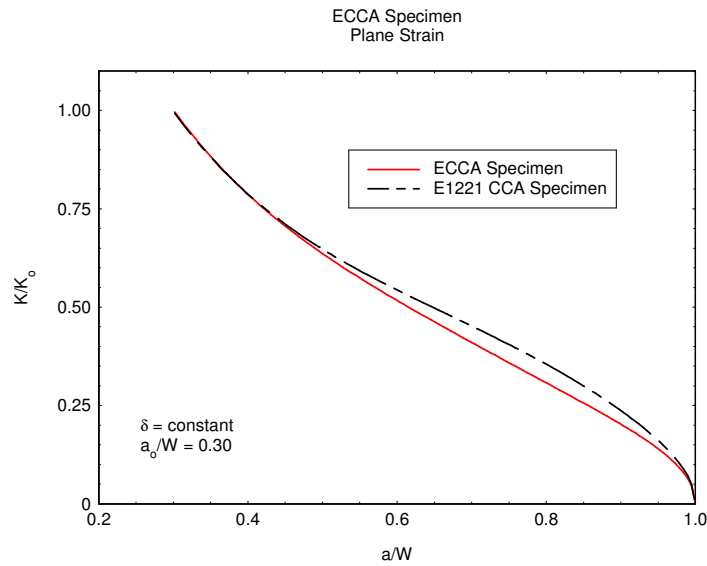


Figure 7 Normalized stress intensity factor as a function of crack size for the standard E1221 compact crack arrest (CCA) specimen and the ECCA specimen, under fixed displacement conditions.

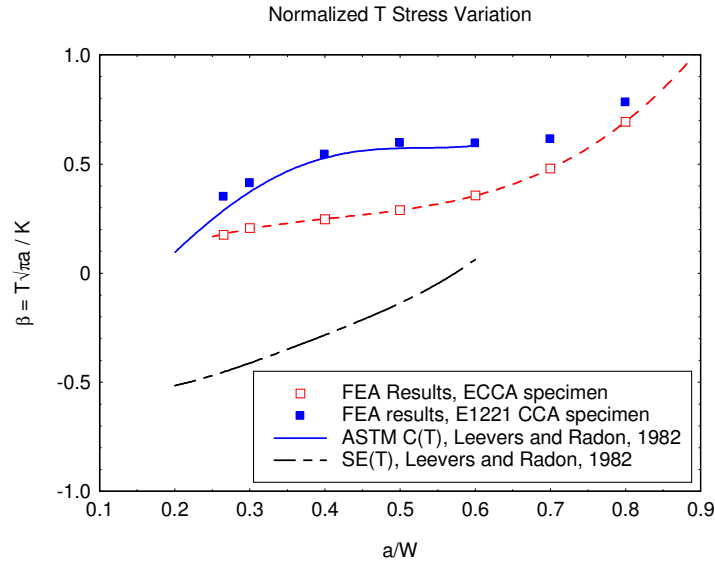


Figure 8 T stress calculations for the standard and extended compact crack arrest specimen geometries, compared with the C(T) and SE(T) specimens [10].

3.3 Dynamic analysis of ECCA specimen

A finite element simulation of a crack arrest test including dynamic crack propagation and arrest was performed to assess the magnitude of the dynamic effects in the ECCA specimen. A 3-D, quarter-symmetric model composed of 17925 elements and 22206 nodes was developed and analyzed using WARP3D. There were five layers of elements through the thickness of the model and the sidegrooves were included in the model as well. The element size along the direction of crack propagation was $l/W = 0.006$. The material was modeled using a piecewise linear, elastic-plastic stress-strain curve including viscoplastic response. Dynamic crack propagation was simulated by progressively releasing the displacement constraints at the crack front to enforce a prescribed crack speed during the propagation event. The crack speed was 380 m/s which is a value typically observed in crack arrest tests of high strength steels [11][12]. The dynamic crack driving force, K_{ID} , was computed from J integral values obtained using the domain integral procedures available in WARP3D.

The crack driving force history computed from the simulation is compared with a quasi-static analysis in Figure 9. The dynamic response of the ECCA specimen is very similar to that of the CCA specimen reported elsewhere [6]. At crack arrest, the static and dynamic stress intensity values are in very close agreement and the dynamic stress intensity oscillates about the final quasi-static value after crack arrest. These results demonstrate that the dynamic effects in the ECCA specimen are no more severe than those observed in the CCA specimen and that a quasi-static analysis is suitable for the ECCA specimen.

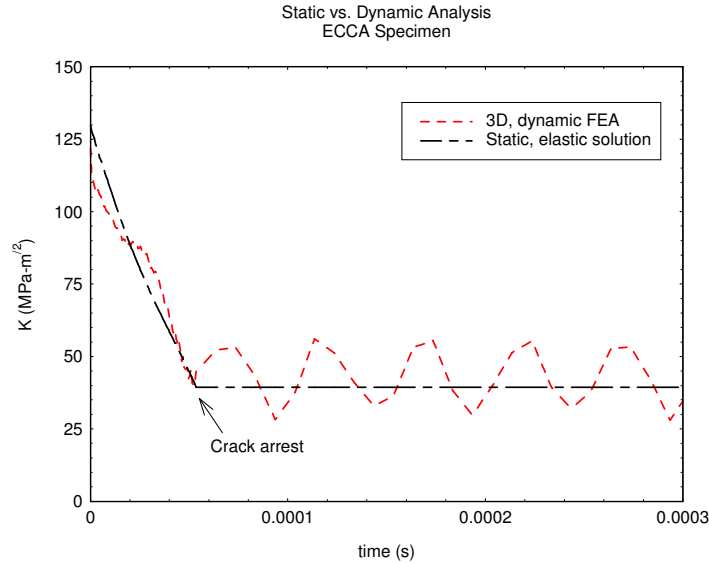


Figure 9 Comparison of quasi-static and dynamic crack driving force as a function of time for the ECCA specimen.

4.0 Experimental Validation

Standard CCA specimens and ECCA specimens were fabricated from a 25mm thick HY-100 steel plate for comparative testing. The crack arrest behavior of this plate has been extensively characterized in prior investigations [13]. The reference temperature, T_0 , corresponding to a median fracture initiation toughness of $100 \text{ MPa}\cdot\text{m}^{1/2}$ was -120°C . All of the specimens were 1T plan size with $W=51\text{mm}$ and $B=25\text{mm}$. The specimens were precracked a minimum of 1.5mm from the notch with a final $\Delta K < 18 \text{ MPa}\cdot\text{m}^{1/2}$. The initial crack lengths were in the range $0.32 \leq a/W \leq 0.39$. The CCA specimens tended towards the longer initial crack sizes as this had been demonstrated to help mitigate the crack leaving the crack plane. The specimens had 10% deep sidegrooves machined on each face. All of the tests reported here were conducted at a temperature of -120°C .

None of the specimens of either geometry exhibited any crack branching or deviation from the initial crack plane. Only one of the five CCA specimens and two of the ECCA specimens yielded valid crack arrest values because the crack grew too far in all of the other cases. In order to meet the requirements of ASTM E1221, the final crack size must be greater than $0.85W$ (or 43.3 mm for these specimens) and most of the tests did not meet this requirement. The results of the tests are summarized in Table 1.

The overall success rate of all of the tests was only 30% which is very poor. It should be noted that the arrested crack lengths in the ECCA specimen were generally shorter than the CCA specimen, even when the initiation values were higher which points to a slight improvement in performance. Tests not

reported herein were attempted at -105°C but none of the specimens arrested the cracks.

Table 1 Summary of results from crack arrest tests of HY-100 steel specimens tested at -120°C.

Specimen ID	Type	K_i (MPa-m ^{1/2})	a_f (mm)	K_{Qa} or K_{Ia}^* (MPa-m ^{1/2})
8	CCA	98.7	45.1	34.2
9	CCA	87.0	38.0	47.6*
11	CCA	107.7	49.1	22.2
207	CCA	110.8	48.2	0.0 ¹
208	CCA	113.7	51.0	0.0 ²
239	ECCA	109.1	45.3	28.4
240	ECCA	120.3	43.6	36.3
241	ECCA	74.6	31.5	45.2*
242	ECCA	102.0	37.3	46.0*
243	ECCA	122.2	46.2	25.7

* denotes valid according to ASTM E1221

¹ clip gage fell out during test, no value available

² crack ran thru specimen, no arrest

5.0 Conclusions

An extended compact crack arrest specimen was developed that reduced the T stress by approximately 50% compared with the standard ASTM E1221 compact crack arrest specimen. Compliance and stress intensity factor calibration functions were presented for precracking via a pin-loaded configuration and for crack arrest testing using a split-pin, wedge-loaded configuration. A dynamic finite element simulation of the crack propagation and arrest in this specimen showed that the dynamic behavior is similar to that of the standard compact crack arrest specimen, thereby justifying the use of a quasi-static analysis to calculate the crack arrest fracture toughness. Experimental tests confirmed that crack arrest values obtained from the ECCA specimen were comparable to those from the CCA specimen although the success rate for both specimen geometries was poor.

6.0 References

- [1] ASTM E1221-06, Standard Test Method for Determining Plane Strain Crack Arrest Toughness, K_{Ia} of Ferritic Steels, ASTM Annual Book of Standards, v03.01, ASTM International, W. Conshohocken, 2008.
- [2] Pussegoda, L.N., Malik, L., Morrison, J., "Measurement of crack arrest fracture toughness of a ship steel plate," J Test Eval, 26(3),(1998) 187-197

- [3] Burch, I.A., Ritter, J.C., Saunders, D.S., Underwood, J.H. Crack arrest fracture toughness testing of naval construction steels, *J Test Eval*, 26(3) (1998) 269-276
- [4] Barker, D.B., Chona, R., Fourney, W.L., and Irwin, G.R., A Report on the Round-Robin Program Conducted to Evaluate the Proposed ASTM Standard Test Method for Determining the Plane Strain Crack Arrest Fracture Toughness, K_{Ia} , of Ferritic Materials, NUREG/CR-4996, U.S. Nuclear Regulatory Commission, Washington, D.C., (January 1988)
- [5] Crosley, P. B., Fourney, W. L., Hahn, G. T., Hoagland, R. G., Irwin, G.R., and Ripling, E. J., Final Report on Cooperative Test Program on Crack Arrest Toughness Measurements, *NUREG/CR-3261*, U.S. Nuclear Regulatory Commission, Washington, D.C. (April 1983)
- [6] Kalthoff, J.F., Beinert, J., Winkler, S., and Klemm, W., Experimental Analysis of Dynamic Effects in Different Crack Arrest Test Specimens, in *Crack Arrest Methodology and Applications*, ASTM STP 711, G.T. Hahn and M.F. Kanninen, Eds., American Society for Testing and Materials (1980) 109-127
- [7] Link, R.E., Analysis of Dynamic Fracture and Crack Arrest of an HSLA Steel in an SE(T) Specimen, *J ASTM Int'l* 3(1) (2006) Paper ID JAI13236
- [8] A.S. Gullerud, K.C. Koppenhoefer, A. Roy, R.H. Dodds, Jr., Warp3D: 3-D Dynamic Nonlinear Fracture Analysis of Solids Using Parallel Computers and Workstations, Report No. UILU-ENG-95-2012, University of Illinois (February 2004)
- [9] ASTM E399-06, Standard Test Method for Linear Elastic Plane Strain Fracture Toughness, K_{Ic} of Metallic Materials, ASTM Annual Book of Standards, v03.01, ASTM International, W. Conshohocken (2008)
- [10] Leever, P.S. and Radon, J.C.D., Inherent stress biaxiality in various fracture specimens, *Int. J. Fract.* 19(4) (1982) 311-325
- [11] Berger, J.R., Dally, J.W., deWitt, R. and Fields, R.J., A Strain Gage Analysis of Fracture in Wide Plate Tests of Reactor Grade Steel, *J Press Ves Tech* Vol. 115 (1993) 398-405
- [12] Link, R.E. and Roe, C., Crack Arrest Testing Using Small Wide Plate SE(T) Specimens, *J ASTM Int'l*, 5(3) (2008) Paper ID JAI101001.
- [13] Link, R.E., Joyce, J.A., and Roe, C., Crack Arrest Testing of High Strength Structural Steels for Naval Applications, submitted to *Eng. Frac. Mech.*